
This item was submitted to [Loughborough's Research Repository](#) by the author.
Items in Figshare are protected by copyright, with all rights reserved, unless otherwise indicated.

Hydrothermal carbonisation of anaerobic digestate for hydro-char production and nutrient recovery

PLEASE CITE THE PUBLISHED VERSION

<https://doi.org/10.1016/j.jece.2021.107027>

PUBLISHER

Elsevier

VERSION

AM (Accepted Manuscript)

PUBLISHER STATEMENT

This paper was accepted for publication in the journal Journal of Environmental Chemical Engineering and the definitive published version is available at <https://doi.org/10.1016/j.jece.2021.107027>.

LICENCE

CC BY-NC-ND 4.0

REPOSITORY RECORD

Roy, Uttam, Tanja Radu, and Jonathan Wagner. 2021. "Hydrothermal Carbonisation of Anaerobic Digestate for Hydro-char Production and Nutrient Recovery". Loughborough University.
<https://hdl.handle.net/2134/17237501.v1>.

1 **Hydrothermal carbonisation of anaerobic digestate for hydro-char production and**
2 **nutrient recovery**

3 Uttam K. Roy¹, Tanja Radu^{1*} and Jonathan Wagner^{2*}

4 *¹School of Architecture, Building and Civil Engineering*

5 *²Department of Chemical Engineering*

6 *Loughborough University, Epinal way, Loughborough, Leicestershire, UK, LE11 3TU*

7 *Corresponding Author Tanja Radu (T.Radu@lboro.ac.uk) and Jonathan Wagner

8 (J.L.Wagner@lboro.ac.uk)

9 **Abstract**

10 This study investigates the potential of hydrothermal carbonisation (HTC) for fractionating
11 anaerobic digestate of sewage sludge into carbon-rich hydrochar and nutrient-rich aqueous
12 phase (AP). AP is subsequently used to supplement cultures of the alkali halophilic
13 microalgae *D. tertiolecta* (CCAP 19/30), to convert sodium bicarbonate into sodium
14 carbonate solution as part of an integrated biogas purification system.

15 HTC at 200°C gave the highest hydrochar yields (78%) and solid carbon retentions (75%),
16 indicating high carbon capture potential. In contrast, the essential growth nutrients nitrogen,
17 phosphorus and sulphur were partially solubilised, resulting in HTC-AP concentrations
18 between 11 times (S) and 50 times (P) higher than those in artificial growth medium. Trace
19 nutrient concentrations in the AP were 10 to 80 times higher compared to the artificial
20 medium, with minimal heavy metal solubilisation.

21 *Dunaliella tertiolecta* grew successfully and without inhibition at HTC-AP concentrations up
22 to 2% (produced at 200°C). AP-supplemented cultures achieved higher cell concentrations
23 (up to 10.0×10^6 cells mL⁻¹), biomass content (maximum of 1.14 ± 0.06 g L⁻¹) and
24 bicarbonate-to-carbonate conversion (83% and 80%, for 1% and 2% of HTC-AP) than the
25 control cultures. Therefore, HTC-AP appears to be a suitable artificial growth medium
26 substitute for cultivating alkali-halophilic microalgae to regenerate carbonate and produce
27 algae biomass, providing an added-value product.

28 **Keywords**

29 Hydrothermal carbonisation, nutrient recovery, anaerobic digestion, carbon capture
30 microalgae cultivation, hydrochar

31 **1. Introduction**

32 Hydrothermal carbonisation (HTC) has attracted significant interest for the treatment and
33 separation of wet biomass residues (*e.g.*, sewage sludge or anaerobic digestate) into stabilised
34 hydrochar, nutrient-rich aqueous phase (AP) products and reaction gases [1,2]. Unlike
35 pyrolysis-based treatments, HTC operates at lower temperatures (180 – 250 °C), avoids the
36 need for energy-intensive drying, and reduces the formation of toxic organic by-products,
37 reducing the cost of downstream processing [3]. During HTC, water acts both as solvent and
38 catalyst, and enables the recovery of inorganic biomass compounds (nutrients) into the liquid
39 phase [4]. Conventional methods of sewage sludge and anaerobic digestate treatment often
40 require energy intensive drying followed by incineration or landfilling, which also results in
41 loss of valuable nutrients. Direct spreading on land requires pasteurisation and is often
42 problematic due to the presence of pollutants and trace elements in residues.

43 The carbon-rich hydrochar could be used as soil improver, bio adsorbent for environmental
44 remediation, novel carbon nanomaterial, or solid fuel source [5,6]. Moreover, stabilised
45 hydrochar can act as a carbon sink, presenting a potential route for long-term carbon
46 sequestration to offset emissions from other sectors [7–9]. However, widespread adoption of
47 this technology has been limited by the treatment and disposal of the HTC-AP, which contains
48 high amounts of ammonium nitrogen, organic carbon, as well as solubilised minerals and
49 metals from the biomass feed. Due to its high nutrient content, the HTC-AP could be used as
50 a natural fertiliser [10], but direct land application is limited by the presence of potential toxic
51 and inhibitory components such as cyclic oxygen and nitrogen compounds and heavy metals.
52 Therefore, different methods have been proposed for the recovery of these nutrients, including
53 chromatographic separation, membrane filtration, nano filtration or bio electrochemical
54 systems (BES) [11].

55 Alternatively, the HTC-AP could be used directly as a nutrient source for microalgae or
56 cyanobacteria cultures as part of an integrated biorefinery concept to yield valuable metabolites
57 and bulk algal biomass for conversion into fuels and chemicals [12–14]. As well as utilising
58 the essential nutrients from the HTC-AP, algae can metabolise the organic waste stream
59 components to enable safe disposal of the treated water stream. A potential application is our
60 recently developed algae-based biogas purification and carbon capture process, which
61 combines anaerobic digestion (AD) of biomass with a two-stage CO₂ absorption and algae
62 cultivation system to yield net carbon-negative biomethane fuel and algae by-product [15]. The
63 system employs sodium carbonate to absorb biogas CO₂, before the resulting bicarbonate
64 solution is used as a carbon source for algae growth to regenerate the CO₂ absorbent [16–18].
65 HTC of the anaerobic digestate can be used to convert the non-digestible biomass fraction into
66 hydrochar for long-term carbon capture whilst recovering essential nutrients for algae growth.

67 The efficiency of the HTC process for the production of hydrochar and recovery of nutrients
68 to the AP depends both on the quality of the feedstock (e.g., waste biomass or AD-digestate),
69 and the reaction time and temperature [19]. High nutrient recovery to the water phase is
70 desirable if the AP is used as fertiliser but must be balanced against the formation of water-
71 soluble organics, which could inhibit algae growth. Several studies have already demonstrated
72 the cultivation of different microalgae strains in the HTC-AP from anaerobic digestate derived
73 from agricultural wastes [20], food wastes [14], and sewage sludge [20,22]. However, all
74 studies have been conducted in freshwater media, whereas our algae-based biogas purification
75 and carbon capture process operates at high salt loading, requiring alkali-halophilic strains such
76 as *D. tertiolecta* (CCAP 19/30). Another key consideration is the distribution of carbon to the
77 hydrochar, AP and gas phase, respectively, to achieve high carbon capture and prevent the
78 accumulation of organic compounds within the algae photobioreactor.

79 Therefore, the current study focuses on the hydrothermal carbonisation of anaerobic digestate
80 (derived from sewage sludge) into carbon-rich hydrochar and nutrient-rich AP. The alkali-
81 halophilic microalgae *D. tertiolecta* (CCAP 19/30) was selected for growth studies in the HTC-
82 AP, due to its ability of converting sodium bicarbonate into the carbonate absorbent required
83 for biogas purification. HTC treatment of dewatered digestate was conducted at three different
84 temperatures to assess the distribution of carbon, macro- and micronutrients to the different
85 product phases. *D. tertiolecta* CCAP 19/30 was cultivated with different concentrations of
86 HTC-AP to evaluate the suitability of this HTC-AP for substituting the artificial growth
87 medium.

88 **2. Materials and methods**

89 **2.1 Materials and algae species**

90 The inoculum (from a long-term operating anaerobic digester), and organic feedstock (sewage
91 sludge) were collected from the Wanlip Sewage Treatment Works (Wanlip STW) plant
92 (Leicester, UK). Inoculum and sewage sludge feedstock were stored at 5 °C prior to use. *D.*
93 *tertiolecta* (CCAP 19/30) was obtained from the Culture collection of Algae and Protozoa
94 (CCAP, Scotland, UK). All reagents, compounds, and Inductivity Coupled Plasma (ICP) metal
95 standards were purchased from Fisher Scientific (UK).

96 **2.2 Anaerobic digestion of sewage sludge and pre-processing of AD-digestate**

97 Anaerobic digestion (AD) of sewage sludge was carried out in 10 L continuous stirred tank
98 reactors (9 L working volume), inoculated with 8.5 L of microbial culture and 0.5 L of fresh
99 sewage sludge. Reactors were fed daily by removing 0.5 L of AD-digestate and replacing it
100 with fresh sewage sludge, maintaining hydraulic retention time (HRT) of 18 days, and organic
101 loading rate (ORL) of 3.5g VS L⁻¹ day⁻¹. Reactors were maintained at 37 °C under continuous
102 vertical stirring (100 rpm). After establishing stable biogas production, AD-digestate removed
103 from the reactors was collected over a period of five consecutive days, mixed and centrifuged
104 (10000xg, 20 min, room temperature) to increase the solid loading of the material. The
105 centrifuged AD-digestate was divided into equal fractions and stored at 5 °C until further
106 processing.

107 **2.3 Hydrothermal carbonisation (HTC) of AD-digestate**

108 HTC reactions were conducted using a 300 mL high-pressure stainless-steel reactor (Model
109 4560, Parr Instrument). Each treatment used approximately 100 g of centrifuged AD-digestate
110 with a total solid content of 11.27%. Once the desired reaction temperature was reached (200,
111 220 or 240 °C), the temperature was maintained for 1 hour, before cooling the reactor in

112 ambient air. Reaction gases were collected into an inverted measuring cylinder to determine
113 the HTC gas yields. Hydrochar and reaction water were separated by gravity filtration using
114 Whatman filter paper (Cole-Parmer, UK), followed by further washing of the hydrochar with
115 deionised water. The solid residue was dried at 105 °C and stored at -20 °C, while the AP and
116 wash water fractions were stored at 4 °C for further use and analysis. The HTC treatment of
117 solid AD-digestate at each temperature was performed in duplicate (n = 2).

118 **2.4 Analysis of AD-digestate and HTC products**

119 The total solid (TS) and moisture contents were determined by drying the samples in a
120 convection drying oven at 105 °C (± 1 °C), followed by cooling in a desiccator for 10 minutes
121 to determine the relative weight loss [23]. The ash content was determined by heating the dried
122 samples inside a muffle furnace (550 °C, 3 h) following the National Renewable Energy
123 Laboratory procedure [24]. The volatile solid content (VS) was calculated as the difference
124 between the TS and ash content of each sample. Each sample was analysed in triplicate (n=3).
125 The total carbon (C), hydrogen (H) and nitrogen (N) content of the dry AD-digestate and hydro-
126 char samples was measured by elemental analysis (Thermo Scientific™ FLASH 1112 series
127 CHN analyser). Volatile oxygen content was calculated by subtracting the ash, carbon,
128 hydrogen and nitrogen content from 100.

129 The S, P and metal contents of the solid (hydrochar and solid AD-digestate) and liquid samples
130 (HTC-AP) were determined on an Inductivity Coupled Plasma–Optical Emission Spectrometer
131 (ICPE-9000, Shimadzu) following the operating procedure described by Zand *et al.* [25]. While
132 the aqueous samples were analysed directly, the solid samples were digested in acid in a
133 temperature and pressure-controlled microwave assisted digestion system (CEM MARS 5 with
134 XP-1500 vessels). Briefly, 0.5 g of oven-dried sample was mixed with 10 mL of a 1:3 mixture
135 of concentrated nitric acid (70% trace analysis grade, Fisher Scientific) and hydrochloric acid

136 (36% trace analysis grade, VWR International). Following microwave digestion (20 min), the
137 samples were made up to 50 mL with deionised water. Multi-element calibration solutions
138 were prepared at different concentration levels (1 – 1000 $\mu\text{g L}^{-1}$) from the single element
139 (1000 mg L^{-1}) ICP grade standards (Fisher, UK), to produce four-point calibration curves for
140 each element ($r^2 = 0.9999$).

141 The total carbon (TC) and total inorganic carbon (TIC) contents in the AP were measured using
142 a Rosemount Dohrmann DC-190 high temperature TOC Analyser (Teledyne Tekmar, USA),
143 by direct injection of the sample (50 μL). The total organic carbon (TOC) was calculated as
144 the difference between the TC and TIC. Ammonium (NH_4^+), nitrate (NO_3^-) and phosphate
145 (PO_4^{3-}) concentrations were determined using Hach-Lange colorimetry test cuvettes (LCK302,
146 LCK338, LCK350, Hach-Lange, Germany).

147 **2.5 Culturing of *Dunaliella tertiolecta* with HTC-AP**

148 *D. tertiolecta* (1×10^5 cells mL^{-1}) from the exponential phase of cell growth (6th day of culture)
149 were inoculated into 200 mL of Modified Johnson medium (J/I) (7.4 mM $\text{MgCl}_2 \cdot 6\text{H}_2\text{O}$,
150 2.0 mM $\text{MgSO}_4 \cdot 7\text{H}_2\text{O}$, 2.7 mM KCl, 1.4 mM $\text{CaCl}_2 \cdot 2\text{H}_2\text{O}$, 9.9 mM KNO_3 , 0.29 mM KH_2PO_4 ,
151 8.9 μM $\text{FeCl}_3 \cdot 6\text{H}_2\text{O}$, 4.8 μM Na_2EDTA , 9.9 μM H_3BO_3 , 0.31 μM $(\text{NH}_4)_6\text{Mo}_7\text{O}_{24} \cdot 4\text{H}_2\text{O}$,
152 0.24 μM $\text{CuSO}_4 \cdot 5\text{H}_2\text{O}$, 0.21 μM $\text{CoCl}_2 \cdot 6\text{H}_2\text{O}$, 0.29 μM ZnCl_2 and 0.20 μM $\text{MnCl}_2 \cdot 4\text{H}_2\text{O}$),
153 supplemented with 11.68 g L^{-1} NaCl (0.2 M) and 1.21 g L^{-1} Tris-HCl (3.0 mM), adjusted to pH
154 of 8 (Roy *et al.*, 2021). Cultures were grown in glass flasks (0.25 L) placed in an orbital shaker
155 incubator with continuous shaking (100 rpm) at 20 °C (± 2 °C) under light-emitting diode
156 (LED) irradiation (12 kLux, mixture of cool and warm white) with a light: dark cycle of 16:8 h.
157 Cultures were mixed with 34 g L^{-1} of sodium bicarbonate (NaHCO_3), to monitor the
158 performance of the cultures to regenerate carbonate for CO_2 absorption [15]. To evaluate the

159 efficiency of cell growth within the HTC-AP, small concentrations of HTC water (1 – 3%)
160 obtained at HTC temperatures of 200 °C (1%, 2%, 3%), 220 °C (1%) and 240 °C (1%) were
161 added to the J/I medium prior to inoculation. The cultures were sampled every two days (1.2
162 ml samples) for cell counting, chlorophyll and carotenoid assay analysis. At the end of the
163 growth cycle (12 days), cells were harvested by centrifugation (4000xg, 4 °C, 10 min) and
164 dried in a convection oven for 24 h at 105 ± 1 °C to determine culture biomass content. All
165 experiments were carried out in biological triplicate (n=3).

166 **2.6 Determination of growth rate, doubling time, and cell density**

167 Cell numbers in the cultures were counted using an improved Neubauer Haemocytometer
168 (Weber, UK). Diluted cell suspensions were treated with 8 µL of 2% formalin solution, before
169 0.010 mL of sample was slowly added so that it spread evenly into each chamber. The total
170 number of cells was calculated using Equation 1. Specific growth rates (μ) and doubling times
171 (t_d) of all cultures were calculated according to the Equations 2 and 3 [15,26].

$$172 \text{ Cell density (Cells mL}^{-1}\text{)} = \text{Number of cells per square} \times \text{dilution factor} \times 10^4 \quad (1)$$

$$173 \text{ Specific growth rate: } \mu = \frac{(\ln n_2 - \ln n_1)}{(t_2 - t_1)} \quad (2)$$

$$174 \text{ Doubling time: } t_d = \frac{\ln 2}{\mu} \quad (3)$$

175 Where n_2 and n_1 were the numbers of cells at time t_2 and t_1

176 **2.7 Determination of total chlorophyll content**

177 After harvesting fresh cells (1 mL culture) by centrifugation (4000xg, 4 °C, 10 min), acetone
178 solution (85%v/v, 1 mL) was added to the pellet and homogenised in extracting solution using
179 a vortex mixer. After separation of the supernatant by centrifugation (14000xg, 4 °C, 10 min),

180 the absorbance was taken at 480, 647, and 664 nm against a blank of 85% acetone solution
181 using a spectrophotometer (Jenway 6305, UK). Total chlorophyll content in the extract (μg
182 mL^{-1}) was calculated using equations 4 – 7 [15].

$$183 \text{ Carotenoid (Car) } (\mu\text{g mL}^{-1}) = 4 \times (\text{Abs}_{480}) \quad (4)$$

$$184 \text{ Chlorophyll a (Chl a) } (\mu\text{g mL}^{-1}) = (12.25 \times \text{Abs}_{664}) - (2.55 \times \text{Abs}_{647}) \quad (5)$$

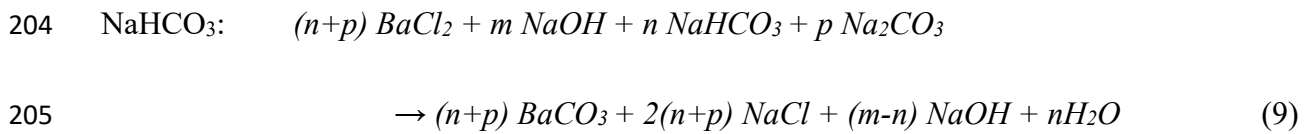
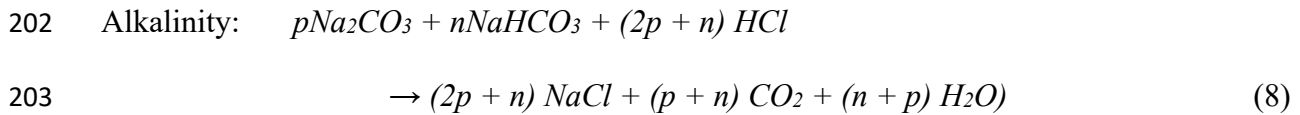
$$185 \text{ Chlorophyll b (Chl b) } (\mu\text{g mL}^{-1}) = (20.31 \times \text{Abs}_{647}) - (4.91 \times \text{Abs}_{664}) \quad (6)$$

$$186 \text{ Total Chlorophyll } (\mu\text{g mL}^{-1}) = (\text{Chl a}) (\mu\text{g mL}^{-1}) + (\text{Chl b}) (\mu\text{g mL}^{-1}) \quad (7)$$

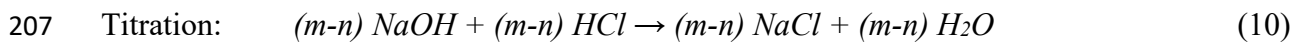
187 Where, Abs_{480} , Abs_{647} and Abs_{664} are the absorbance of the acetone extract measured at 480,
188 647, 664 nm respectively.

189 **2.8 Determination of NaHCO_3 and Na_2CO_3 content**

190 Carbonate/bicarbonate contents were determined according to Jain and Mehta (1980). Total
191 alkalinity (complete conversion of NaHCO_3 and Na_2CO_3 into CO_2 , Equation 8) was determined
192 by mixing 1 mL of centrifuged culture supernatant (3000xg, 15 min) with 3 mL of
193 decarbonised water (boiled to remove dissolved CO_2) prior to titration with 0.1M HCl to a
194 methyl orange end point (pH 4.3). The NaHCO_3 content was determined by mixing another
195 1 mL of centrifuged culture supernatant with 3mL of decarbonised water and 4 mL of 0.1M
196 NaOH before adding 2 mL of 0.48M BaCl_2 solution and phenolphthalein indicator (2 drops).
197 The mixture was titrated with 0.1M HCl to the indicator endpoint (loss of pink colour at pH
198 8.3). The net amount of alkali used (m-n) corresponds to the bicarbonate (HCO_3^-) content of
199 the sample, resulting in the formation of carbonate, which is subsequently precipitated as
200 barium carbonate (Equations 9 and 10). The carbonate content was thus determined by
201 subtracting the bicarbonate content from the total alkalinity of the sample [15].



206 Where $m > n$, amount $BaCl_2 > n+P$



208 3. Results and Discussion

209 3.1 Feedstock characterisation

210 The anaerobic digestate used in this study was collected from a continuous sewage sludge fed
 211 AD reactor, as described above. During AD, 60.5% of volatile solids were converted into
 212 biogas, causing a significant reduction in both the VS and TS concentrations in the AD-
 213 digestate (Table 1). In contrast, the concentrations of non-volatile solids remained the same,
 214 resulting in an increase in the ash content of the dried solids from 17.4 % to 33.9%. The high
 215 ash content of the digestate results in relatively low concentrations of carbon (35.2%) and
 216 hydrogen (5.1%), while the nitrogen content of the digestate (4.3%) is slightly higher than in
 217 the sewage sludge (4.20 ± 0.06), as during AD, unlike hydrogen and carbon, most of the
 218 nitrogen in the sewage sludge remains in the anaerobic digestate phase (rather than the gas
 219 phase). As previously reported, most of this nitrogen is in the form of proteins and other cell
 220 components from the microbial AD community, together with unconverted ammonium present
 221 in sewage sludge [28].

222 To increase the solid concentrations of the AD-digestate, it was centrifuged prior to the HTC
 223 experiments to remove excess water. Low solid loadings can result in reduced product yields,
 224 increase the energy requirements of the reaction, and increase the amount of water that needs

225 to be treated after the reaction. The final solid loadings of 10.8% are in the range of typical
 226 hydrothermal conditions. Centrifugation of the digestate had little impact on its ash content and
 227 elemental composition, indicating minimal loss of solids to the supernatant (liquid) phase
 228 (estimated as 3.2% based on difference in TS and VS content).

229 *Table 1 Properties of feedstock used for hydrothermal carbonisation*

Parameter	Sewage sludge (Feed stock)	AD-digestate	Centrifuged digestate
Moisture content (% WW)	92.39 ± 0.42	96.24 ± 0.02	89.22 ± 0.72
TS (% WW)	7.61 ± 0.42	3.76 ± 0.02	10.78 ± 0.72
Volatile solid (% WW)	6.29 ± 0.43	2.48 ± 0.01	7.34 ± 0.19
Ash content (% DW)	17.43 ± 0.96	33.92 ± 0.17	32.26 ± 3.66
C (%)	43.51 ± 0.89	35.19 ± 0.61	35.48 ± 0.37
H (%)	6.59 ± 0.15	5.14 ± 0.08	5.24 ± 0.04
N (%)	4.20 ± 0.06	4.25 ± 0.06	4.90 ± 0.02
O (%)	27.54 ± 0.92	21.56 ± 0.59*	22.12 ± 1.85*

230 *WW – wet weight, DW – dry weight*

231 **Oxygen calculated by difference*

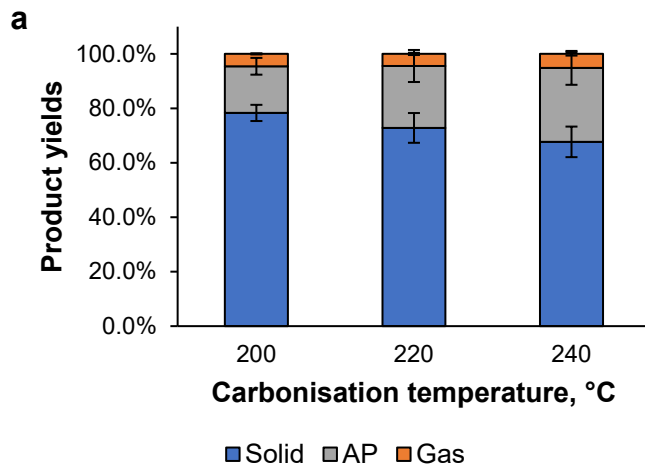
232 In addition to the CHN content, the concentrations of other growth nutrients (P, S, Na, K, Ca,
 233 Mg, Fe, B, Zn, Co, Cu, Mo) present in the modified Johnson medium, as well as metals (Al,
 234 Cr, Cd, Pb, Sr, Ni, Bi, Ba) were determined to investigate their partitioning to the AP during
 235 HTC reactions. Amongst these, the highest concentrations were observed for Ca (40.5 mg g⁻¹),
 236 P (37.7 mg g⁻¹), Fe (20.8 mg g⁻¹), sulphur (17.9 mg g⁻¹) and Al (16.5 mg g⁻¹), while the
 237 concentrations of heavy metals (Bi, Pb, Cr, Cd) were all below 0.1 mg g⁻¹ (Table 2).

238 3.2 Carbonisation of AD-digestate

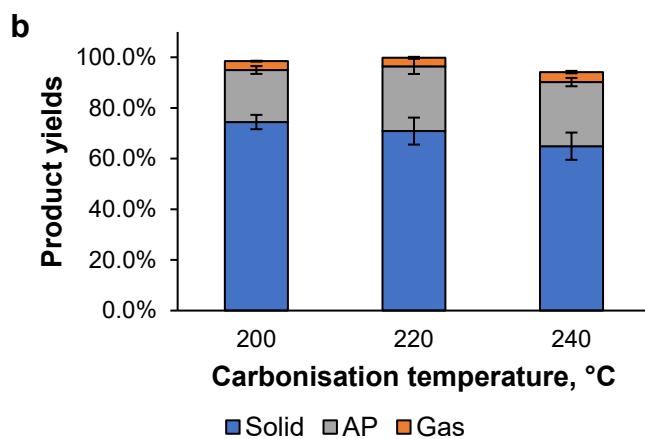
239 The HTC reaction temperatures used in this study (200 °C, 220 °C and 240 °C) are based on
240 the range of typical HTC temperatures (180 – 250 °C), which generally represent a compromise
241 between carbon retention to the hydrochar, and volatilisation of hydrogen and oxygen to
242 produce a stable solid residue. HTC reaction products were separated into three separate
243 phases: solid hydro-char, AP, and gas products. As HTC gas products are known to consist
244 predominantly of CO₂ (with minor amounts of CO, H₂ and CH₄) the gas yields were calculated
245 by assuming a molecular weight of 44 g mol⁻¹ [29]. AP yields are difficult to measure directly
246 due to the loss of volatile organics during AP drying, and hence were calculated as the
247 difference between biomass feed and solid and gas yields (Figure 1a). As expected, hydrochar
248 was recovered as the major reaction products, with yields up to 78.3% (± 3.0%) at the lowest
249 reaction temperature of 200 °C. In line with previous studies [30,31], solid yields reduced as
250 the reaction temperature was increased (72.8% ± 5.5% and 67.7% ± 5.6% at 220 °C and
251 240 °C, respectively), which may be associated with the slow reaction kinetics at the lower
252 temperature [32]. Gas yields remained constantly low between 4.4% and 5.1% (± 0.2 – 0.6%),
253 suggesting reaction gases are mostly formed below 200 °C. Therefore, the reduction in solid
254 yields at higher temperatures is expected to correspond to the increased production of water-
255 soluble reaction products, as observed previously [33].

256 In addition to the overall mass balance, the carbon and nitrogen distributions to the three
257 product phases were determined. Unlike the overall mass balance, C and N distribution to the
258 AP were measured directly using the concentrations obtained from TC and colorimetric (NH₄⁺
259 and NO₃⁻) analysis, and the volume of recovered water. The carbon distribution closely matches
260 the overall mass distribution, with a slight reduction in solid (1.9 – 3.9%) and gas recovery (1.0
261 – 1.2%) and a corresponding increase in the AP yields (Figure 1b). Hydrothermal conditions

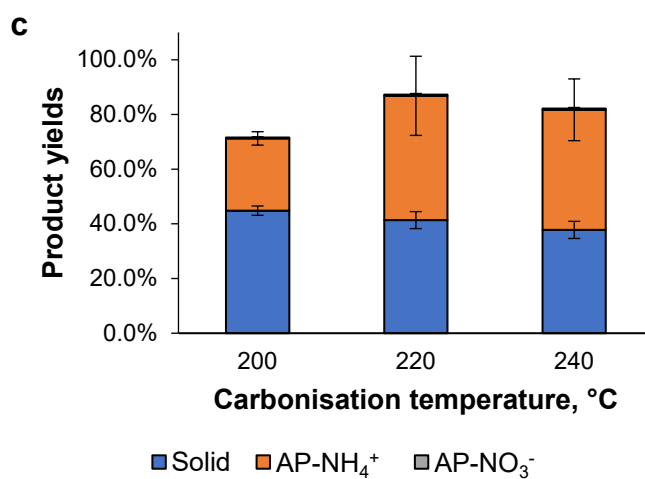
262 preferably solubilise smaller compounds with higher H/C and O/C ratios, leading to lower
263 hydrogen and oxygen retention in the solid. Therefore, the differences between the total mass
264 balance and the carbon balance indicate a high retention of inorganic minerals within the solid
265 hydrochar product, corresponding to low metal loadings in the AP product. The overall carbon
266 mass balance closure ranges from 94.2% to 99.9%, indicating minimal losses throughout the
267 extraction process. However, the water recovery from the reactor ranged from only 51.2% to
268 59.7%, demonstrating significant water losses during product collection and separation,
269 presumably through evaporation. As these losses did not affect the overall carbon balance, the
270 water-soluble carbon products appear to be relatively non-volatile and concentrate in the
271 retained water.



272



273



274

275 *Figure 1: Product yields from hydrothermal carbonisation of digestate. (a) total mass*
 276 *balance; (b) carbon distribution; (c) nitrogen distribution.*

277 Unlike carbon, the nitrogen recovery to hydrochar accounted for only 37.8 – 44.8% (± 1.7 –
 278 3.1%) of nitrogen in the digestate, reducing with increasing reaction temperature (Figure 1c).

279 This result is consistent with previous studies showing that nitrogen retention in the hydrochar
280 continues to reduce up to temperatures of 270 °C [34,35]. Proteins in the digestate feed start to
281 degrade at 150 °C via hydrolysis and cracking reactions to form ammonia (which dissolves in
282 water to form ammonium, NH_4^+) and organic nitrogen compounds, which mostly distribute to
283 the AP [36]. Ammonia in the HTC-AP accounts for 26.4% to 45.5% ($\pm 1.1 - 3.9\%$) of initial
284 nitrogen, while the yields of nitrate are low ($< 0.5\%$) at all temperatures. Although biomass
285 degradation could also cause the formation of nitrites (NO_2^-), their yields tend to be even lower
286 than those of nitrates and were not determined in this study [35]. Overall nitrogen balance
287 closure significantly increases from 71.6% at 200 °C to 87.3% at 220 °C, consistent with the
288 decomposition of organic nitrogen compounds in the AP to form ammonia. The missing
289 nitrogen may also be attributed to the evaporation of ammonia during the extraction process,
290 in line with the significant losses of water during the extraction. Process scale-up and
291 continuous processing of the reaction products are expected to significantly reduce these losses,
292 leading to improved nitrogen recovery to the AP.

293 **3.3 Characterisation of hydrochar**

294 HTC of the centrifuged digestate resulted in a significant increase in solid ash content from
295 32.3% to between 47.9 and 49.4% (Table 2). The remaining volatile matter (VM) content (51
296 – 52%) is similar or higher than those obtained during previous HTC studies of AD-digestates
297 (34.5% - 52%) [29,37,38], but lower than the values from direct carbonisation of sewage sludge
298 (57.4 – 63.0%) [31,39]. These differences can be explained by variations in reaction conditions
299 (*e.g.*, reaction time, temperature, and solid loading), as well as differences in the composition
300 of the feed material. For example, anaerobic digestion of sewage sludge results in a significant
301 decrease in VM content, as the volatile material is converted into biogas, increasing the ash
302 content of these samples prior to HTC.

303 Carbon content in the hydrochar remained relatively constant, regardless of HTC temperature,
304 (33.7% – 34.5%), only slightly lower than the carbon content in the centrifuged digestate
305 (35.5%). These results show the preferential retention of carbon (over H, N and O) within the
306 reducing solid organic fraction, indicating the formation of larger, carbon-rich compounds,
307 such as polycyclic aromatics. In contrast, HTC caused a much higher relative decrease of the
308 hydrogen, nitrogen and particularly oxygen contents, resulting in a significant reduction in the
309 H/C (0.147), N/C (0.138) and O/C (0.624) ratios of the centrifuged digestate. The H/C ratios
310 of the hydrochar reduced with increasing carbonisation temperature (0.128, 0.125 and 0.119 at
311 200, 220, and 240 °C, respectively), consistent with previous results for the carbonisation of
312 wood [30], digestate [32] and active sewage sludge [31]. This may indicate an increase in the
313 rate of the dehydration reaction (removal of hydroxy groups to form H₂O), or preferential loss
314 of shorter hydrocarbons with higher H/C ratios at higher temperatures. The N/C ratios remained
315 relatively constant (0.080 – 0.083), suggesting that most of the excess nitrogen is solubilised
316 at temperatures below 200 °C, while additional nitrogen losses are proportional to the overall
317 decrease in hydrochar yields at increased HTC temperatures. Finally, the O/C ratios increase
318 from 0.290 to 0.326 as the reaction temperature is raised from 200 °C to 240 °C. The oxygen
319 content of the digestate feed is mostly reduced via decarboxylation (release of CO₂),
320 decarbonylation (release of CO) and dehydration reactions (removal of hydroxy groups to form
321 H₂O) at temperatures above 150 °C [31]. Therefore, the increase in O/C ratio with increased
322 HTC temperature suggests that most of these deoxygenation reactions occur below 200 °C,
323 consistent with the constant gas yields observed at all studied HTC temperatures. Instead, the
324 remaining oxygen appears to incorporate preferentially into heavy char products, resulting in
325 the release of shorter hydrocarbons with high H/C and low O/C ratios.

326

327 *Table 2: Elemental compositions of AD-digestate and solid HTC reaction products*

Parameter	Centrifuged Digestate	HC200	HC220	HC240
<i>Proximate and ultimate analyses (% w/w)</i>				
Ash content	32.26 ± 3.66	49.35 ± 0.61	47.89 ± 0.03	48.08 ± 0.07
*C	35.48 ± 5.10	33.72 ± 0.57	34.53 ± 1.12	34.01 ± 0.12
*H	5.24 ± 0.057	4.34 ± 0.062	4.33 ± 0.157	4.07 ± 0.012
*N	4.89 ± 0.035	2.80 ± 0.003	2.78 ± 0.044	2.73 ± 0.026
P	3.77	5.64	5.16	4.47
S	1.79	2.09	1.76	1.43
**O	22.12 ± 1.85	9.79	10.47	11.10
<i>Metal concentration (mg g⁻¹)</i>				
Al	16.51	24.27	23.07	23.21
B	0.157	0.251	0.228	0.137
Ba	0.443	0.708	0.642	0.586
Bi	0.089	0.78	0.241	0.080
Ca	40.5	53.9	55.6	51.5
Cd	0.005	0.008	0.006	0.005
Co	0.010	0.015	0.012	0.013
Cr	0.073	0.114	0.114	0.107
Cu	0.445	0.464	0.587	0.574
Fe	20.8	35.34	34.9	32.6
K	7.27	4.56	4.48	4.41
Mg	5.63	14.0	11.4	10.6
Mn	0.269	0.580	0.479	0.404
Mo	0.054	0.320	0.145	0.052
Na	2.51	1.12	1.33	1.38
Ni	0.042	0.107	0.108	0.092
Pb	0.087	0.175	0.136	0.119
Si	0.88	0.647	0.630	0.492
Sr	0.206	0.312	0.287	0.264
Zn	0.767	0.152	0.229	0.974

328 **From Elemental CHN analysis*

329 ***Oxygen calculated by difference*

330 Comparing ICP analysis results for the three hydrochar products to centrifuged digestate shows
 331 a substantial increase in the concentrations of most metals in the reaction solids, in line with

332 the increase in ash content. Based on the ICP analysis of the AP, the calculated recoveries of
333 Cu, Al, Ca, Fe, Ba, Mn, and Sr to the hydrochar exceed 98% at all three reaction temperatures.
334 The lowest metal recoveries are seen for Cd (50.2 – 61.0%), Bi (56.1 – 57.7 %), Mo (62.3 –
335 64.8%) and Co (70.8 – 73.7%), but all four elements are present at very low initial
336 concentrations ($<0.1 \text{ mg g}^{-1}$). The high metal recoveries are consistent with literature results
337 and can be explained by the presence and formation of water-insoluble metal oxides, minerals
338 (e.g., carbonates and phosphates), and interaction of different minerals to form metal
339 complexes [40–43]. Accordingly, the recoveries of phosphorus (93.2 – 94.1%) and sulphur
340 (80.9 – 82.9%) are also high. Phosphorus can form a range of different molecular moieties (for
341 example, organic phosphates, orthophosphate, phosphonate and polyphosphate) which may
342 associate with the minerals present in the digestate feed to form water-insoluble precipitates,
343 or be adsorbed onto the rough and uneven surfaces of the hydrochar [42,44,45]. Relatively low
344 recoveries are seen for sodium (69.6 – 72.5%) and potassium (65.1 – 69.1%), reducing slightly
345 with an increase in reaction temperature, in line with the overall decrease in hydrochar yields.
346 Both elements form a large number of water-soluble salts and are an important component of
347 the algal growth medium used in this study.

348 **3.4 Composition of HTC-AP**

349 The AP produced by HTC treatment of AD-digestate at different temperature was dark in
350 colour and the recovered amount of water increased with increasing reaction temperature
351 (Table 3). While its inorganic carbon content increased with increasing reaction temperature
352 (0.80 to 1.71 g L^{-1}), the organic carbon content reduced by a similar amount (16.01 to
353 14.68 g L^{-1}), giving an approximately constant total carbon concentration. These results can be
354 explained by the increased solubility and hydrolysis of biochemical compounds such as
355 polysaccharides, cellulose, hemicellulose and lignin at temperatures above $190 \text{ }^\circ\text{C}$ into sugars,
356 sugar derivatives and other intermediates [32,46]. Further reactions of these intermediates

357 cause the formation of a wide range of water-soluble organic compounds, including acetic acid,
358 propionic acid, butanoic acids, aldehydes, furans, pyrroles, pyrazines, pyridines, 3-
359 methylbenzofurane and 5-methyl-2-furancarboxyaldehyde [39], as well as deoxygenated
360 compounds with low water solubility, which partition to the hydrochar phase. While some of
361 these organic products could act as a carbon source for mixotrophic algae growth, compounds
362 such as phenols, furans, and phenolics are known growth inhibitors and may be toxic to algae
363 growth [10]. Colorimetric analysis of the AP showed that most of the inorganic nitrogen was
364 in the form of ammonium (NH_4^+), while the formation of nitrates (NO_3^-) was low. Ammonia
365 can be formed by the cleavage of peptide bonds, deamination and ring opening reactions and
366 commonly accounts for > 95% of total AP nitrogen [3,35]. Raising the reaction temperature
367 from 200 to 220 °C resulted in a significant increase in ammonium concentrations from 3.89
368 to 7.36 g L⁻¹, consistent with earlier studies [34,46,47]. At 240 °C, AP ammonium
369 concentration slightly reduced to 5.80 g L⁻¹, potentially due to increased evaporation of
370 ammonia. In contrast, the modified Johnson medium used for the cultivation of *D. tertiolecta*
371 contains mostly nitrates (0.614 g L⁻¹) corresponding to a nitrogen concentration of 0.18 g L⁻¹.
372 Based on these results, the nitrogen concentration in the HTC AP is 16.7 to 31.6 times higher
373 than the nitrogen concentration in the modified Johnson medium and could therefore substitute
374 a significant portion of this macronutrient.

375 The total phosphorus concentration (determined by ICP analysis) in the HTC-AP remained
376 relatively constant between 0.434 and 0.459 g L⁻¹. However, as the water recovery increases at
377 higher temperatures, the overall P recovery to the AP increased slightly from 5.9% at 200 °C
378 to 6.7% at 240 °C, consistent with previous studies on HTC of AD-digestate [34,46]. Unlike
379 total phosphorus, the phosphate (PO_4^{3-}) concentration (by colorimetric analysis) was found to
380 increase from 0.71 g L⁻¹ at 200 °C to 1.28 and 1.20 g L⁻¹ at 220 and 240 °C, respectively,
381 corresponding to 51%, 96% and 85% of total phosphorus in the AP. Phosphorus in the HTC

382 AP can be attributed to the decomposition of complex organic phosphorus containing
383 compounds (for instance, phospholipids, DNA and phosphates monoesters), forming PO_4^{3-} and
384 organic phosphorus compounds [28]. Therefore, the results suggests that most of the AP
385 phosphorus was solubilised at the lowest HTC temperature, while organic intermediates
386 continued to react to form phosphates as the final reaction product. Despite the relatively low
387 overall recovery of phosphorus to the HTC-AP, the P concentrations are ~50 times higher than
388 the phosphorus concentrations in the Johnson medium. This shows that small quantities of the
389 HTC-AP should be sufficient to meet the phosphorus demand for the algae culture.

390 The sulphur concentration in the AP reduced from 0.71 to 0.55 g L⁻¹ when increasing the
391 reaction temperature from 200 to 240 °C, corresponding to a 2.2% reduction in overall sulphur
392 recovery. Most of the sulphur (80.9 to 82.9%) partitioned into the hydrochar, more than twice
393 the sulphur retention observed during HTC of sewage sludge (40%) [36]. Nonetheless, these
394 values exceed the sulphur concentrations in the modified Johnson medium by a factor of 8.5 to
395 11.0 and should therefore be sufficient to meet the algae culture sulphur requirements.

396

397 *Table 3: Concentrations of growth nutrients and trace metals in HTC-AP products and*
 398 *modified Johnson medium*

Parameter	AP200	AP220	AP240	Johnson medium
Water recovery (%)	53.3	51.2	59.7	<i>n/a</i>
Total organic carbon (g L ⁻¹)	16.06	15.36	14.68	<i>n/a</i>
Total inorganic carbon (g L ⁻¹)	0.80	1.37	1.71	4.86*
<i>From colorimetric analysis (g L⁻¹)</i>				
NH ₄ ⁺	3.89 ± 0.33	7.36 ± 3.13	5.80 ± 1.41	0.034
NO ₃ ⁻	0.16 ± 0.08	0.27 ± 0.17	0.21 ± 0.12	0.614
PO ₄ ³⁻	0.71 ± 0.28	1.28 ± 0.62	1.20 ± 0.60	0.028
<i>From ICP analysis (mg L⁻¹)</i>				
S	710	595	545	64.1
P	453	434	459	8.98
Na	140	129	132	4598
K	482	443	460	504
Ca	26.4	20.5	24.3	56.1
Mg	5.75	22.6	59.5	228
Fe	29.3	12.1	6.00	0.497
Mo	2.20	2.15	2.20	0.21
Mn	0.35	0.35	0.45	0.011
B	8.70	7.20	7.30	0.107
Zn	1.45	0.85	1.05	0.019
Co	0.35	0.30	0.30	0.012
Cu	bdl	bdl	bdl	0.015
Al	5.90	6.60	7.25	<i>n/a</i>
Cr	0.80	0.60	0.40	<i>n/a</i>
Cd	0.25	0.2	0.25	<i>n/a</i>
Pb	1.10	1.05	1.10	<i>n/a</i>
Sr	0.40	0.35	0.35	<i>n/a</i>
Ni	0.80	0.70	0.65	<i>n/a</i>
Bi	4.15	4.15	4.15	<i>n/a</i>
Ba	0.50	0.75	0.40	<i>n/a</i>

399 * Inorganic carbon concentration based on bicarbonate feed concentration of 34 g L⁻¹

400 The highest metal concentrations in the AP were found for potassium (443 – 460 mg L⁻¹) and
401 sodium (129 – 140 mg L⁻¹), which are both essential components of Johnson medium.
402 Relatively high concentrations were also found for Ca (20.5 – 26.4 mg L⁻¹) and Mg (5.75 –
403 59.5 mg L⁻¹), but in both cases the concentrations are lower than in the growth medium. In
404 contrast, the concentrations of other trace nutrients are between 10 (Mo) to 80 (B) times higher
405 than in the medium, except for copper, which could not be detected by ICP analysis. The
406 concentrations of heavy metals were found to be very low, mostly below 1 mg L⁻¹, except for
407 Bi, which reached concentrations of ~4 mg L⁻¹.

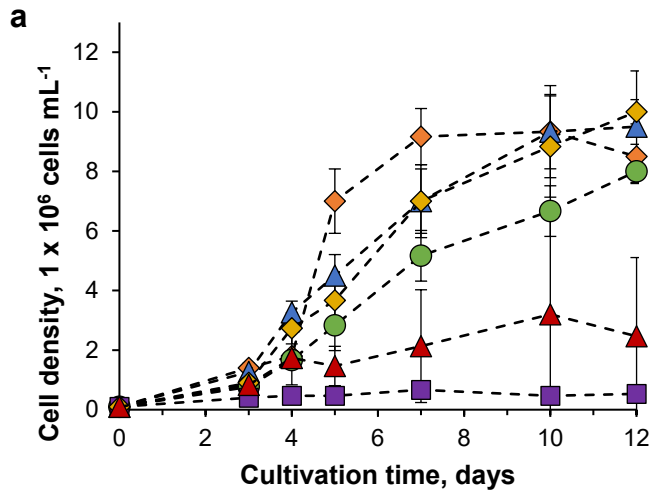
408 Metal concentrations (except Fe and Cr) in the AP generally increased with increasing reaction
409 temperature, indicating increased transformation of metals into dissolved ions under
410 hydrothermal carbonisation [40]. Similar trends were previously observed for Cd and Pb [48],
411 Cr [41] and K, Ca, Al and Mn [49].

412 **3.5 Cultivation of *Dunaliella tertiolecta* in HTC-AP**

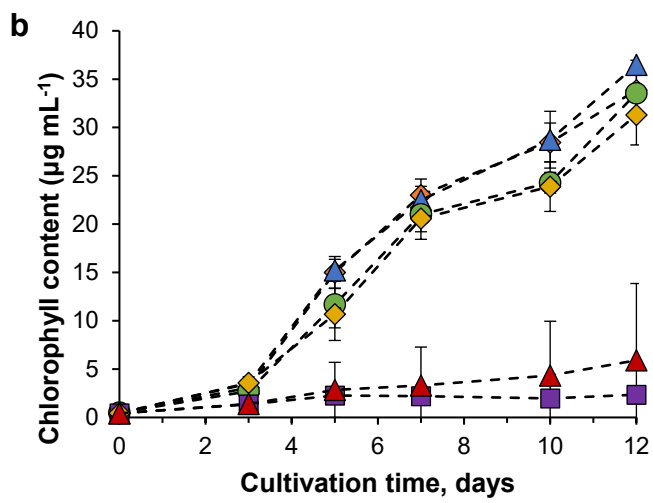
413 The presence of high concentrations of C, N, P, K, S, and metals (Ca, Mg, Fe) in the HTC-AP
414 demonstrates that nutrients are solubilised and transferred from the AD-digestate to the water
415 phase during carbonisation treatment. Nutrient concentrations in the HTC aqueous phases were
416 several folds higher (up to 80-fold) than required for cultivating *D. tertiolecta*, based on the
417 composition of modified Johnson medium (culture medium, Table 3). Therefore, the diluted
418 HTC-AP may be suitable for cultivating this strain, similar to earlier studies with freshwater
419 algae [50–52]. Adding low concentrations of HTC-AP has minimum impact on the colour of
420 the growth medium and is therefore unlikely to impact light attenuation, affecting algae growth.
421 However, the HTC-AP also contains high concentrations of organic carbon (up to 16.1 g L⁻¹),
422 which may inhibit algal growth. Previous studies employed high dilutions of the AP products
423 (50 – 200 fold) to reduce the inhibitory effect of toxic compounds for algae culturing

424 [14,22,50–52]. Therefore, initial screening studies were conducted to explore the compatibility
425 of *D. tertiolecta* with the AP obtained at the three different HTC temperatures at concentrations
426 up to 3% in modified Johnson medium (Figure 2).

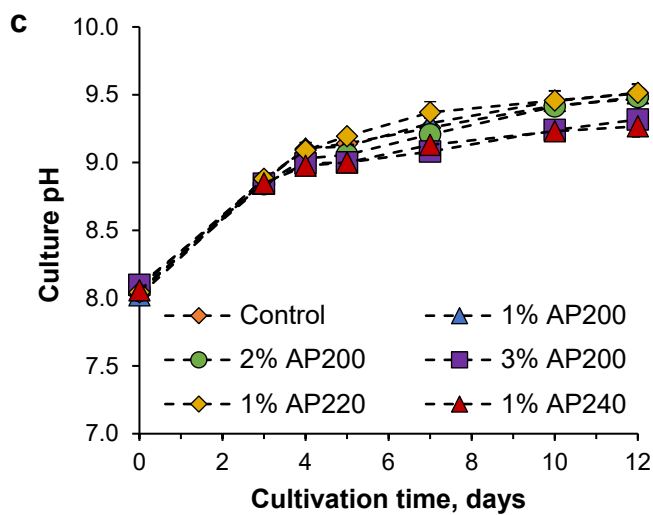
427 Growth curves for all cultures (including the control) displayed an initial lag phase of up to
428 three days, which may be due to the cell's acclimatisation to the culture medium [13]. The
429 highest exponential growth rates ($0.95 \pm 0.13 \text{ d}^{-1}$) were obtained for cells grown with 1%
430 AP200, slightly higher than the growth rates obtained in the control. Increasing the AP
431 concentration from 1% to 3% or increasing HTC temperature from 200 to 240 °C, both resulted
432 in a significant reduction in growth rate and final cell densities, indicating significant growth
433 inhibition. Cells grown with the control medium reached the stationary phase after seven days,
434 with a maximum cell density of $8.50 \times 10^6 \text{ cells mL}^{-1}$, before cell concentrations started to
435 decline after 10 days of cultivation, potentially due to nutrient limitations [13]. In contrast, cell
436 densities in cultures grown with 1% and 2% of AP200 and 1% AP220 continued to increase
437 after 7 days, with maximum cell densities obtained with 1% AP220 ($10.0 \times 10^6 \text{ cells mL}^{-1}$). As
438 the AP products were added to the algae growth medium, total nutrient concentrations in the
439 mixed media were increased, which may explain the higher maximum algae concentrations
440 compared to the control.



441



442



443

444 *Figure 2: Cultivation of Dunaliella tertiolecta with different concentrations of HTC-AP (a)*

445 *Algae growth curves; (b) Chlorophyll content in the cultures; (c) Culture pH.*

446 The highest biomass contents were found in cultures grown with 1% AP200 ($1.14 \pm 0.06 \text{ g L}^{-1}$)
 447 ¹) and 1% AP220 ($1.11 \pm 0.08 \text{ g L}^{-1}$), higher than those in the control ($1.01 \pm 0.04 \text{ g L}^{-1}$),
 448 demonstrating that the addition of HTC-AP to the culture medium can improve the production
 449 of biomass (Table 4). Cell concentrations are in line with previous growth studies of *Chlorella*
 450 sp. ($0.64 - 1.5 \text{ g L}^{-1}$) [13,22,50,52], although most of these studies diluted the AP in water,
 451 rather than growth medium. Ash content, total chlorophyll and carotenoid content were
 452 relatively similar in all cultures, except for the cultures grown with 3% AP200 and 1% AP240,
 453 which displayed much higher ash content and lower chlorophyll and carotenoid contents.

454 *Table 4 Proximate analysis of D. tertiolecta biomass grown with HTC-AP*

	Control	1% AP200	2% AP200	3% AP200	1% AP220	1% AP240
Growth rate (μ, d^{-1})	0.80 ± 0.17	0.95 ± 0.13	0.63 ± 0.17	0.26 ± 0.05	0.71 ± 0.08	0.62
Biomass content (g L^{-1})	1.01 ± 0.04	1.14 ± 0.06	1.05 ± 0.04	0.28 ± 0.08	1.11 ± 0.08	0.355
Ash content (%)	20.74 ± 0.31	21.13 ± 5.14	20.19 ± 5.08	47.29 ± 8.06	19.15 ± 4.94	23.00 ± 5.98
Chlorophyll content (mg g^{-1} biomass)	33.59 ± 2.62	31.95 ± 0.51	31.91 ± 2.88	2.34 ± 0.20	28.29 ± 3.43	16.65
Carotenoid content (mg g^{-1} biomass)	8.47 ± 1.15	7.64 ± 0.44	8.04 ± 1.12	1.24 ± 0.20	6.63 ± 0.86	3.60

455 To evaluate the health of the different algae cultures, the accumulation of chlorophyll in each
 456 culture was determined (Figure 2b). Cultures with higher chloroplastic pigments in the cells
 457 can absorb more light energy, which is subsequently converted into chemical energy resulting
 458 in higher cell densities [53]. In line with the growth curves, the fastest increase in chlorophyll
 459 content was observed for the control and 1% AP200 cultures, followed by the 2% AP200 and
 460 1% AP220 cultures. In contrast, much lower chlorophyll concentrations were detected for cells
 461 in the 1% AP240, and particularly the 3% AP200 media, explaining the low cell concentrations
 462 obtained for these cultures, and indicating significant inhibition for these experiments.

463 *D. tertiolecta* is known for its high tolerance to heavy metals and its ability to remove metals
464 from the culture medium [54–56]. Therefore, given the low concentrations of metals in the
465 diluted HTC-AP products ($< 0.1 \text{ mg L}^{-1}$) and similar metal concentrations in the AP200, AP220
466 and AP240 products (two of which did not display inhibition), it is unlikely that the observed
467 inhibition can be attributed to the presence of heavy metals. Similarly, the concentrations of
468 ammonium in the mixed media were low (0.117 g L^{-1} for 3% AP200 and 0.058 g L^{-1} for 1%
469 AP240) and comparable to the concentration of the 1% AP220 experiment (0.074 g L^{-1}),
470 therefore unlikely to be the cause of the observed inhibition [52]. Instead, the inhibition is likely
471 to be caused by the presence of organic compounds such as hydroxy methyl furfural (HMF),
472 furfural, phenol or formic acid, produced during the carbonisation of biomass $>190 \text{ }^\circ\text{C}$
473 [39,44,57,58]. HMF and furfural ($\sim 1 \text{ mM}$) can delay the growth of algae, whilst concentrations
474 above 7 mM can completely inhibit algal growth by blocking electron transfer in the
475 photosynthetic electron transport system [14,59]. Although the total organic carbon content in
476 the HTC-AP from the current study was relatively independent of temperature, higher
477 temperatures can increase the conversion of water-soluble intermediates, such as amino acids
478 and sugars, into more toxic secondary products, increasing their inhibitory effect on algae
479 cultivation. The results from the growth studies suggest that the concentrations of these
480 inhibitors are significantly lower in the AP200 and AP220 products but increasing their
481 concentration above a certain threshold (3%) still results in significant growth inhibition.

482 **3.6 Effect of HTC-AP supplementation on carbonate regeneration by *Dunaliella***

483 *tertiolecta*

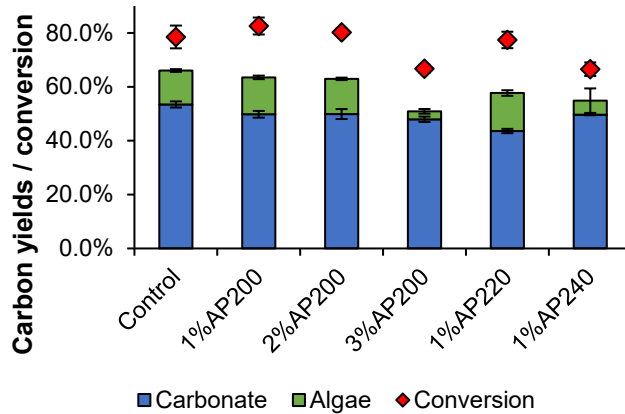
484 The main objective of culturing *D. tertiolecta* in our recently developed algae-based biogas
485 purification and carbon capture process [15] is the conversion of sodium bicarbonate
486 (NaHCO_3) into sodium carbonate (Na_2CO_3) to regenerate the CO_2 absorbent required for

487 biogas purification. First, bicarbonate ions are used by the algae to produce CO₂ required for
488 algae growth ($\text{HCO}_3^- + \text{H}^+ \rightarrow \text{CO}_2 + \text{H}_2\text{O}$). The consumption of protons causes the culture pH
489 to increase, resulting in the deprotonation of bicarbonate to regenerate the original carbonate
490 ions ($\text{HCO}_3^- + \text{OH}^- \rightarrow \text{CO}_3^{2-} + \text{H}_2\text{O}$).

491 Based on our earlier study, cultures were supplemented with a bicarbonate concentration of
492 34 g L⁻¹, corresponding to a carbon loading of 4.86 g L⁻¹. Carbonate and bicarbonate
493 concentrations were monitored throughout the growth cycle and the final carbon distribution
494 was determined after 12 days of cultivation, by multiplying the algae yield with the algae
495 carbon content (Figure 3). As expected, bicarbonate concentrations reduced in all six
496 cultivation experiments, together with an increase in carbonate concentrations. The highest
497 bicarbonate conversions were obtained for cultures grown with 1% and 2% AP200 (83% and
498 80%, respectively), higher than the conversion achieved in the control. In contrast, conversions
499 were significantly reduced in the cultures grown in 3% AP200 and 1% AP240, indicating a
500 clear link between bicarbonate conversion and algae carbon yields. Despite the big differences
501 in algae growth between the cultures with different AP loadings, trends in culture pH were very
502 similar, increasing from around 8.0 at the start of culture to final values between 9.3 to 9.5
503 (Figure 2c). These trends explain the partial conversion of bicarbonate to carbonate, even for
504 the cultures where algae growth was poor.

505 Carbonate yields ranged between 43.6% for 1% AP220 to 53.5% for the control, while the
506 carbonate yields of the cultures in 1% and 2% AP200 and 1% AP240 were within 0.5% of the
507 theoretical yields of 50%. Algae accounted for up to 14.1% of the converted bicarbonate
508 carbon, resulting in a significant discrepancy between the converted bicarbonate carbon and
509 carbon partitioned to algae and carbonate products of up to 49.1% for the culture in 3% AP200.
510 This unaccounted carbon may be attributed to the loss of excess CO₂ to the atmosphere,

511 indicating the importance of maintaining fast algae growth to achieve a high degree of carbon
512 capture.



513

514 *Figure 3: Bicarbonate conversion and carbon distribution to carbonate and algae products*
515 *from cultivation of *Dunaliella tertiolecta* with different concentrations of HTC-AP*

516 4. Conclusion

517 This study investigated the potential of hydrothermal carbonisation to fractionate sewage
518 sludge derived AD digestate into carbon-rich hydrochar and nutrient-rich aqueous phase, to
519 supplement the cultivation of *D. tertiolecta* as part of an integrated biogas purification system.
520 HTC resulted in high hydrochar mass and carbon yields of up to 78% and 75%, respectively,
521 together with high retention of metals within the solid, leading to low heavy metal
522 concentrations in the HTC-AP. Although most of the phosphorus and nitrogen partitioned to
523 the solid phase, AP concentrations were up to 11 times (S) and 50 times (P) higher than their
524 concentrations in artificial algal growth medium. Similarly, concentrations of trace nutrients
525 were between 10 and 80 times higher than in the artificial growth medium. In contrast, HTC
526 solubilised the majority of nitrogen, leading to HTC-AP nitrogen concentrations between 17 to
527 32 times those required for algae growth.

528 *D. tertiolecta* was successfully grown without inhibition with HTC-AP concentrations of up
529 to 2%, achieving increased cell concentrations and biomass concentrations compared to the
530 control. These cultures also displayed the highest rates of carbonate regeneration, indicating
531 the feasibility of HTC-AP as nutrient source for integrated biogas purification via alkali-
532 halophilic microalgae. However, significant inhibition was observed for samples obtained
533 above 220°C and at HTC-AP concentrations above 3%, attributed to the presence of organic
534 by-products such as furfurals and phenols, which are known to inhibit algae growth. Further
535 studies are required to optimise HTC reaction conditions (reaction time, reaction temperature,
536 solid loading) and monitor the fate of organic pollutants during microalgae culture.

537 **Acknowledgements**

538 This work was funded jointly by the Engineering and Physical Sciences Research Council
539 (EPSRC) and Department of Transport through a flexible funding grant from the Supergen
540 Bioenergy Network (SGBH FF Feb2019 2). It also used equipment funded by a Research
541 Grant from the Royal Society (RGS\R1\191135).

542 **References**

- 543 [1] A. Urbanowska, M. Kabsch-Korbutowicz, M. Wnukowski, P. Seruga, M. Baranowski,
544 H. Pawlak-Kruczek, M. Serafin-Tkaczuk, K. Krochmalny, L. Niedzwiecki, Treatment
545 of liquid by-products of hydrothermal carbonization (HTC) of agricultural digestate
546 using membrane separation, *Energies*. 13 (2020) 1–12. doi:10.3390/en13010262.
- 547 [2] Y. Shi, G. Luo, Y. Rao, H. Chen, S. Zhang, Hydrothermal conversion of dewatered
548 sewage sludge: Focusing on the transformation mechanism and recovery of
549 phosphorus, *Chemosphere*. 228 (2019) 619–628.
550 doi:10.1016/j.chemosphere.2019.04.109.
- 551 [3] K.R. Parmar, A.B. Ross, Integration of hydrothermal carbonisation with anaerobic

- 552 digestion; Opportunities for valorisation of digestate, *Energies*. 12 (2019).
553 doi:10.3390/en12091586.
- 554 [4] S. Román, J. Libra, N. Berge, E. Sabio, K. Ro, L. Li, B. Ledesma, A. Alvarez, S. Bae,
555 Hydrothermal carbonization: Modeling, final properties design and applications: A
556 review, *Energies*. 11 (2018) 1–28. doi:10.3390/en11010216.
- 557 [5] A. Mohammadi, G. Venkatesh, M. Sandberg, S. Eskandari, K. Granström, Life cycle
558 assessment of combination of anaerobic digestion and pyrolysis: Focusing on different
559 options for biogas use, *Adv. Geosci.* 49 (2019) 57–66. doi:10.5194/adgeo-49-57-2019.
- 560 [6] F. Monlau, C. Sambusiti, E. Ficara, A. Aboulkas, A. Barakat, H. Carrère, New
561 opportunities for agricultural digestate valorization: Current situation and perspectives,
562 *Energy Environ. Sci.* 8 (2015) 2600–2621. doi:10.1039/c5ee01633a.
- 563 [7] S. Malghani, E. Jüschke, J. Baumert, A. Thuille, M. Antonietti, S. Trumbore, G.
564 Gleixner, Carbon sequestration potential of hydrothermal carbonization char
565 (hydrochar) in two contrasting soils; results of a 1-year field study, *Biol. Fertil. Soils*.
566 51 (2015) 123–134. doi:10.1007/s00374-014-0980-1.
- 567 [8] E. Bevan, J. Fu, Y. Zheng, Challenges and opportunities of hydrothermal carbonisation
568 in the UK; Case study in Chirnside, *RSC Adv.* 10 (2020) 31586–31610.
569 doi:10.1039/d0ra04607h.
- 570 [9] M.P. Maniscalco, M. Volpe, A. Messineo, Hydrothermal carbonization as a valuable
571 tool for energy and environmental applications: A review, *Energies*. 13 (2020).
572 doi:10.3390/en13164098.
- 573 [10] L. Leng, J. Li, Z. Wen, W. Zhou, Use of microalgae to recycle nutrients in aqueous
574 phase derived from hydrothermal liquefaction process, *Bioresour. Technol.* 256 (2018)
575 529–542. doi:10.1016/j.biortech.2018.01.121.

- 576 [11] M. Usman, H. Chen, K. Chen, S. Ren, J.H. Clark, J. Fan, G. Luo, S. Zhang,
577 Characterization and utilization of aqueous products from hydrothermal conversion of
578 biomass for bio-oil and hydro-char production: a review, *Green Chem.* 21 (2019)
579 1553–1572. doi:10.1039/C8GC03957G.
- 580 [12] P. Biller, A.B. Ross, S.C. Skill, A. Lea-Langton, B. Balasundaram, C. Hall, R. Riley,
581 C.A. Llewellyn, Nutrient recycling of aqueous phase for microalgae cultivation from
582 the hydrothermal liquefaction process, *Algal Res.* 1 (2012) 70–76.
583 doi:10.1016/j.algal.2012.02.002.
- 584 [13] K. McGaughy, A. Abu Hajer, E. Drabold, D. Bayless, M.T. Reza, Algal Remediation
585 of Wastewater Produced from Hydrothermally Treated Septage, *Sustainability.* 11
586 (2019) 3454. doi:10.3390/su11123454.
- 587 [14] S.Z. Tarhan, A.T. Koçer, D. Özçimen, İ. Gökalp, Cultivation of green microalgae by
588 recovering aqueous nutrients in hydrothermal carbonization process water of biomass
589 wastes, *J. Water Process Eng.* 40 (2021). doi:10.1016/j.jwpe.2020.101783.
- 590 [15] U.K. Roy, T. Radu, J.L. Wagner, Carbon-negative biomethane fuel production:
591 Integrating anaerobic digestion with algae-assisted biogas purification and
592 hydrothermal carbonisation of digestate, *Biomass and Bioenergy.* 148 (2021) 106029.
593 doi:10.1016/j.biombioe.2021.106029.
- 594 [16] C. Zhu, R. Zhang, L. Cheng, Z. Chi, A recycling culture of *Neochloris oleoabundans*
595 in a bicarbonate-based integrated carbon capture and algae production system with
596 harvesting by auto-flocculation, *Biotechnol. Biofuels.* 11 (2018) 1–11.
597 doi:10.1186/s13068-018-1197-6.
- 598 [17] R.L. Zhang, J.H. Wang, L.Y. Cheng, Y.J. Tang, Z.Y. Chi, Selection of microalgae
599 strains for bicarbonate-based integrated carbon capture and algal production system to

- 600 produce lipid, *Int. J. Green Energy*. 16 (2019) 825–833.
601 doi:10.1080/15435075.2019.1641103.
- 602 [18] Z. Chi, Y. Xie, F. Elloy, Y. Zheng, Y. Hu, S. Chen, Bicarbonate-based Integrated
603 Carbon Capture and Algae Production System with alkalihalophilic cyanobacterium,
604 *Bioresour. Technol.* 133 (2013) 513–521. doi:10.1016/j.biortech.2013.01.150.
- 605 [19] I. Idowu, L. Li, J.R.V. Flora, P.J. Pellechia, S.A. Darko, K.S. Ro, N.D. Berge,
606 Hydrothermal carbonization of food waste for nutrient recovery and reuse, *Waste*
607 *Manag.* 69 (2017) 480–491. doi:10.1016/j.wasman.2017.08.051.
- 608 [20] L. Zuliani, N. Frison, A. Jelic, F. Fatone, D. Bolzonella, M. Ballottari, Microalgae
609 cultivation on anaerobic digestate of municipalwastewater, sewage sludge and agro-
610 waste, *Int. J. Mol. Sci.* 17 (2016). doi:10.3390/ijms17101692.
- 611 [21] D.R. Vardon, B.K. Sharma, G. V. Blazina, K. Rajagopalan, T.J. Strathmann,
612 Thermochemical conversion of raw and defatted algal biomass via hydrothermal
613 liquefaction and slow pyrolysis, *Bioresour. Technol.* 109 (2012) 178–187.
614 doi:10.1016/j.biortech.2012.01.008.
- 615 [22] Y.Z. Belete, S. Leu, S. Boussiba, B. Zorin, C. Posten, L. Thomsen, S. Wang, A. Gross,
616 R. Bernstein, Characterization and utilization of hydrothermal carbonization aqueous
617 phase as nutrient source for microalgal growth, *Bioresour. Technol.* 290 (2019)
618 121758. doi:10.1016/j.biortech.2019.121758.
- 619 [23] L. Matsakas, U. Rova, P. Christakopoulos, Evaluation of dried sweet sorghum stalks as
620 raw material for methane production, *Biomed Res. Int.* 2014 (2014).
621 doi:10.1155/2014/731731.
- 622 [24] A. Sluiter, B. Hames, D. Hyman, C. Payne, R. Ruiz, C. Scarlata, J. Sluiter, D.
623 Templeton, J.W. Nrel, Determination of total solids in biomass and total dissolved

- 624 solids in liquid process samples, *Natl. Renew. Energy Lab.* (2008) 3–5.
- 625 [25] N. Zand, B.Z. Chowdhry, F.B. Zotor, D.S. Wray, P. Amuna, F.S. Pullen, Essential and
626 trace elements content of commercial infant foods in the UK, *Food Chem.* 128 (2011)
627 123–128. doi:10.1016/j.foodchem.2011.03.005.
- 628 [26] T.D.P. Nguyen, D.H. Nguyen, J.W. Lim, C.K. Chang, H.Y. Leong, T.N.T. Tran,
629 T.B.H. Vu, T.T.C. Nguyen, P.L. Show, Investigation of the relationship between
630 bacteria growth and lipid production cultivating of microalgae *Chlorella vulgaris* in
631 seafood wastewater, *Energies.* 12 (2019). doi:10.3390/en12122282.
- 632 [27] S. Jain, G. Mehta, Investigation of Sodium Carbonate, Sodium Bicarbonate and Water
633 Systems for Saturated Solar Ponds, U.S. Department of Energy, Warrenton, Virginia,
634 1980.
- 635 [28] C.I. Aragón-Briceño, O. Grasham, A.B. Ross, V. Dupont, M.A. Camargo-Valero,
636 Hydrothermal carbonization of sewage digestate at wastewater treatment works:
637 Influence of solid loading on characteristics of hydrochar, process water and plant
638 energetics, *Renew. Energy.* 157 (2020) 959–973. doi:10.1016/j.renene.2020.05.021.
- 639 [29] N.D. Berge, K.S. Ro, J. Mao, J.R.V. Flora, M.A. Chappell, S. Bae, Hydrothermal
640 carbonization of municipal waste streams, *Environ. Sci. Technol.* 45 (2011) 5696–
641 5703. doi:10.1021/es2004528.
- 642 [30] M.M.L.J.A.R.K.S.K.C.F.A.B.N.D.N.Y. Titirici, K.H.F.C.B.O.K.J. Emmerich,
643 Hydrothermal carbonization of biomass residuals : A comparative review of the
644 chemistry , processes and ... Hydrothermal carbonization of biomass residuals : a
645 comparative review of the chemistry , processes and, *Biofuels.* 2 (2017) 71–106.
- 646 [31] P. Zhao, Y. Shen, S. Ge, K. Yoshikawa, Energy recycling from sewage sludge by
647 producing solid biofuel with hydrothermal carbonization, *Energy Convers. Manag.* 78

- 648 (2014) 815–821. doi:10.1016/j.enconman.2013.11.026.
- 649 [32] M.T. Reza, C. Coronella, K.M. Holtman, D. Franqui-Villanueva, S.R. Poulson,
650 Hydrothermal carbonization of autoclaved municipal solid waste pulp and
651 anaerobically treated pulp digestate, *ACS Sustain. Chem. Eng.* 4 (2016) 3649–3658.
652 doi:10.1021/acssuschemeng.6b00160.
- 653 [33] U. Ekpo, A.B. Ross, M.A. Camargo-Valero, P.T. Williams, A comparison of product
654 yields and inorganic content in process streams following thermal hydrolysis and
655 hydrothermal processing of microalgae, manure and digestate, *Bioresour. Technol.* 200
656 (2016) 951–960. doi:10.1016/j.biortech.2015.11.018.
- 657 [34] Y. Yu, Z. Lei, X. Yang, X. Yang, W. Huang, K. Shimizu, Hydrothermal carbonization
658 of anaerobic granular sludge : E ffect of process temperature on nutrients availability
659 and energy gain from produced hydrochar, *Appl. Energy.* 229 (2018) 88–95.
660 doi:10.1016/j.apenergy.2018.07.088.
- 661 [35] X. Zhuang, Y. Huang, Y. Song, H. Zhan, X. Yin, C. Wu, The transformation pathways
662 of nitrogen in sewage sludge during hydrothermal treatment, *Bioresour. Technol.* 245
663 (2017) 463–470. doi:10.1016/j.biortech.2017.08.195.
- 664 [36] C. He, A. Giannis, J.Y. Wang, Conversion of sewage sludge to clean solid fuel using
665 hydrothermal carbonization: Hydrochar fuel characteristics and combustion behavior,
666 *Appl. Energy.* 111 (2013) 257–266. doi:10.1016/j.apenergy.2013.04.084.
- 667 [37] D. Bhatt, A. Shrestha, R.K. Dahal, B. Acharya, P. Basu, R. MacEwen, Hydrothermal
668 carbonization of biosolids from Waste water treatment plant, *Energies.* 11 (2018) 1–
669 10. doi:10.3390/en11092286.
- 670 [38] P. Saetea, N. Tippayawong, Recovery of Value-Added Products from Hydrothermal
671 Carbonization of Sewage Sludge, *ISRN Chem. Eng.* 2013 (2013) 1–6.

672 doi:10.1155/2013/268947.

673 [39] E. Danso-Boateng, G. Shama, A.D. Wheatley, S.J. Martin, R.G. Holdich,
674 Hydrothermal carbonisation of sewage sludge: Effect of process conditions on product
675 characteristics and methane production, *Bioresour. Technol.* 177 (2015) 318–327.
676 doi:10.1016/j.biortech.2014.11.096.

677 [40] Y.J. Liang, L.Y. Chai, H. Liu, X.B. Min, Q. Mahmood, H.J. Zhang, Y. Ke,
678 Hydrothermal sulfidation of zinc-containing neutralization sludge for zinc recovery
679 and stabilization, *Miner. Eng.* 25 (2012) 14–19. doi:10.1016/j.mineng.2011.09.014.

680 [41] C. He, K. Wang, A. Giannis, Y. Yang, J.Y. Wang, Products evolution during
681 hydrothermal conversion of dewatered sewage sludge in sub- and near-critical water:
682 Effects of reaction conditions and calcium oxide additive, *Int. J. Hydrogen Energy.* 40
683 (2015) 5776–5787. doi:10.1016/j.ijhydene.2015.03.006.

684 [42] R. Huang, Y. Tang, Evolution of phosphorus complexation and mineralogy during
685 (hydro)thermal treatments of activated and anaerobically digested sludge: Insights
686 from sequential extraction and P K-edge XANES, *Water Res.* 100 (2016) 439–447.
687 doi:10.1016/j.watres.2016.05.029.

688 [43] Y. Zhao, Q. Ren, Y. Na, Speciation transformation of arsenic during municipal sewage
689 sludge incineration with cotton stalk as additive, *Fuel.* 202 (2017) 541–546.
690 doi:10.1016/j.fuel.2017.04.074.

691 [44] M. Langone, D. Basso, Process waters from hydrothermal carbonization of sludge:
692 Characteristics and possible valorization pathways, *Int. J. Environ. Res. Public Health.*
693 17 (2020) 1–31. doi:10.3390/ijerph17186618.

694 [45] T. Wang, Y. Zhai, Y. Zhu, C. Peng, T. Wang, B. Xu, C. Li, G. Zeng, Feedwater pH
695 affects phosphorus transformation during hydrothermal carbonization of sewage

- 696 sludge, *Bioresour. Technol.* 245 (2017) 182–187. doi:10.1016/j.biortech.2017.08.114.
- 697 [46] C. Aragón-Briceño, A.B. Ross, M.A. Camargo-Valero, Evaluation and comparison of
698 product yields and bio-methane potential in sewage digestate following hydrothermal
699 treatment, *Appl. Energy*. 208 (2017) 1357–1369. doi:10.1016/j.apenergy.2017.09.019.
- 700 [47] R. Toufiq, A. Freitas, X. Yang, S. Hiibel, H. and Lin, C.J. Coronella, Hydrothermal
701 Carbonization (HTC) of Cow Manure: Carbon and Nitrogen Distributions in HTC
702 Products, *Environ. Prog. Sustain. Energy*. 35 (2016) 1002–1011. doi:10.1002/ep.
- 703 [48] W. Shi, C. Liu, D. Ding, Z. Lei, Y. Yang, C. Feng, Z. Zhang, Immobilization of heavy
704 metals in sewage sludge by using subcritical water technology, *Bioresour. Technol.*
705 137 (2013) 18–24. doi:10.1016/j.biortech.2013.03.106.
- 706 [49] S.X. Sumida H, Y.K. Sumida H, Effects of Hydrothermal Process on the Nutrient
707 Release of Sewage Sludge, *Int. J. Waste Resour.* 03 (2013). doi:10.4172/2252-
708 5211.1000124.
- 709 [50] Z. Du, B. Hu, A. Shi, X. Ma, Y. Cheng, P. Chen, Y. Liu, X. Lin, R. Ruan, Cultivation
710 of a microalga *Chlorella vulgaris* using recycled aqueous phase nutrients from
711 hydrothermal carbonization process, *Bioresour. Technol.* 126 (2012) 354–357.
712 doi:10.1016/j.biortech.2012.09.062.
- 713 [51] S. Zora Tarhan, A.T. Koçer, D. Özçemen, İ. Gökcalp, Utilization of hydrothermal
714 process water for microalgal growth, *Eurasian J. Biol. Chem. Sci.* 3 (2020) 42–47.
- 715 [52] L. Zhang, H. Lu, Y. Zhang, B. Li, Z. Liu, N. Duan, M. Liu, Nutrient recovery and
716 biomass production by cultivating *Chlorella vulgaris* 1067 from four types of post-
717 hydrothermal liquefaction wastewater, *J. Appl. Phycol.* 28 (2016) 1031–1039.
718 doi:10.1007/s10811-015-0640-3.
- 719 [53] W. Gu, H. Li, P. Zhao, R. Yu, G. Pan, S. Gao, X. Xie, A. Huang, L. He, G. Wang,

720 Quantitative proteomic analysis of thylakoid from two microalgae (*Haematococcus*
721 *pluvialis* and *Dunaliella salina*) reveals two different high light-responsive strategies,
722 *Sci. Rep.* 4 (2014) 1–12. doi:10.1038/srep06661.

723 [54] H.A. Qari, I.A. Hassan, Removal of pollutants from waste water using *Dunaliella*
724 algae, *Biomed. Pharmacol. J.* 7 (2014) 147–151. doi:10.13005/bpj/465.

725 [55] K. Miazek, W. Iwanek, C. Remacle, A. Richel, D. Goffin, Effect of metals, metalloids
726 and metallic nanoparticles on microalgae growth and industrial product biosynthesis:
727 A review, *Int. J. Mol. Sci.* 16 (2015) 23929–23969. doi:10.3390/ijms161023929.

728 [56] B. Kutlu, E. Mutlu, Growth and bioaccumulation of cadmium, zinc, lead, copper in
729 *Dunaliella* sp. isolated from Homa lagoon, eastern Aegean Sea, *Indian J. Geo-Marine*
730 *Sci.* 46 (2017) 1162–1169.

731 [57] R. Becker, U. Dorgerloh, E. Paulke, J. Mumme, I. Nehls, Hydrothermal carbonization
732 of biomass: Major organic components of the aqueous phase, *Chem. Eng. Technol.* 37
733 (2014) 511–518. doi:10.1002/ceat.201300401.

734 [58] M. Escala, T. Zumbühl, C. Koller, R. Junge, R. Krebs, Hydrothermal carbonization as
735 an energy-efficient alternative to established drying technologies for sewage sludge: A
736 feasibility study on a laboratory scale, *Energy and Fuels.* 27 (2013) 454–460.
737 doi:10.1021/ef3015266.

738 [59] S. Yu, A. Forsberg, K. Kral, M. Pedersen, Furfural and hydroxymethylfurfural
739 inhibition of growth and photosynthesis in *spirulina*, *Br. Phycol. J.* 25 (1990) 141–148.
740 doi:10.1080/00071619000650131.

741